Running on water: Three-dimensional force generation by basilisk lizards

S. Tonia Hsieh* and George V. Lauder

Department of Organismic and Evolutionary Biology, Harvard University, 26 Oxford Street, Cambridge, MA 02138

Edited by David B. Wake, University of California, Berkeley, CA, and approved October 16, 2004 (received for review August 5, 2004)

Water provides a unique challenge for legged locomotion because it readily yields to any applied force. Previous studies have shown that static stability during locomotion is possible only when the center of mass remains within a theoretical region of stability. Running across a highly yielding surface could move the center of mass beyond the edges of the region of stability, potentially leading to tripping or falling. Yet basilisk lizards are proficient water runners, regularly dashing across bodies of water to evade predators. We present here direct measurements of time-averaged force produced by juvenile plumed basilisk lizards (*Basiliscus plumifrons*) while running across water. By using digital particle image velocimetry to visualize fluid flow induced by foot movement, we show that sufficient support force is generated for a lizard to run across water and that novel strategies are also required to run across a highly yielding surface. Juvenile basilisk lizards produce greatest support and propulsive forces during the first half of the step, when the foot moves primarily vertically downwards into the water; they also produce large transverse reaction forces that change from medial (79% body weight) to lateral (37% body weight) throughout the step. These forces may act to dynamically stabilize the lizards during water running. Our results give insight into the mechanics of how basilisk lizards run across water and, on a broader scale, provide a conceptual basis for how locomotor surface properties can challenge established rules for the mechanics of legged locomotion.

Basiliscus plumifrons | hydrodynamics | particle image velocimetry | locomotion

Running across water is a dramatic example of a locomotor function once thought to be limited to small-bodied invertebrates (e.g., see refs. 1–4). Although considerable literature is available that examines the biomechanics of movement across solid surfaces, very little is known about how softer, more yielding surfaces, such as water, affect legged locomotion. Water provides an unusual challenge, because it readily yields to any applied force. As a result, it would be expected that any animal attempting to walk across water would sink toward the supporting limb.

There are few vertebrates capable of running across water. Waterfowl are known to slap the water with their feet during flapping take-off. However, they obtain a great deal of lift from their wings. Anolis lizards and baby green iguanas have been reported to run short distances across water. This capability, however, seems to be limited primarily to smaller-bodied individuals. Basilisk lizards (*Basiliscus* sp.) are unique in that they regularly run across water, using only their feet as a source of both lift and thrust. This behavior is prevalent among hatchlings through adults and is made more spectacular by their large size range: Hatchlings weigh $\approx$2 g, whereas adults can weigh $>$200 g. Basilisk lizards, therefore, serve as interesting model organisms for examining the mechanics of this remarkable locomotor feat.

A previous study (5, 6) elucidated the mechanics of water running by dropping a circular disk modeling a basilisk foot vertically onto the water surface while measuring the impulses produced at impact and during disk deceleration. Results showed that the initial water contact impulse is small. When combined with impulses theoretically produced during the remainder of the stride, however, small lizards were capable of generating supportive impulses of substantial magnitudes. Juvenile lizards could theoretically generate a maximum total impulse more than twice their body weight, whereas larger lizards could not generate such proportionately large impulses (5). The advantage of this physical model is that it permitted quantification of the impulse produced upon the instant of contact with the water surface, a parameter otherwise only quantifiable by attaching an accelerometer to the lizard's foot. As a purely passive vertical disk drop, however, it does not represent the kinematics of actual basilisk water running, which consists of both propulsive vertical (slap) and horizontal (stroke) phases. These two phases should also generate thrust in addition to lift forces to enable the lizard to run across the water surface. This study quantifies the forces produced after the foot impacts the water to understand how basilisks are able to produce both propulsive thrust and lift during bipedal locomotion on water.

The general goals of this study were to generate new data on the patterns of water flow induced by basilisk foot movement and to provide insight on how a highly yielding surface affects force generation in light of what is known from terrestrial legged locomotion studies. We hypothesized that basilisks support their weight throughout the slap and stroke phases and that most of the forward propulsive force is generated during the stroke when primary motion of the foot is backwards, and when foot angle to the water surface approaches 90° (7). We also expected that basilisks would generate large transverse forces that counteract the tendency for the body to sink and tilt toward the supporting hindlimb.

Materials and Methods

The use of force plates mounted flush to the surface of a track is a well established technique for measuring forces produced during locomotion across solid surfaces (8–10). In contrast, measuring forces exerted by biological surfaces acting in water has proven to be challenging (11, 12). We used digital particle image velocimetry (DPIV; a technique in which a laser light sheet illuminates a thin section of water to permit visualisation of fluid particle movement) to quantify forces produced as lizards ran across water.

Animals. Five juvenile plumed basilisk lizards (*Basiliscus plumifrons*; 11.4–20.0 g) were obtained from a reptile wholesale supplier (Quality Reptiles, Los Angeles). Animals were housed in pairs in 114-liter aquaria and fed a diet of crickets and mealworms dusted with vitamin and calcium supplement. All lizards were deprived of food for a day before trials.

This paper was submitted directly (Track II) to the PNAS office.

Abbreviations: CM, center of mass; DPIV, digital particle image velocimetry.

*To whom correspondence should be addressed at: Museum of Comparative Zoology, Harvard University, 26 Oxford Street, Cambridge, MA 02138. E-mail: sthsieh@oeb.harvard.edu.

www.pnas.org/cgi/doi/10.1073/pnas.0405736101

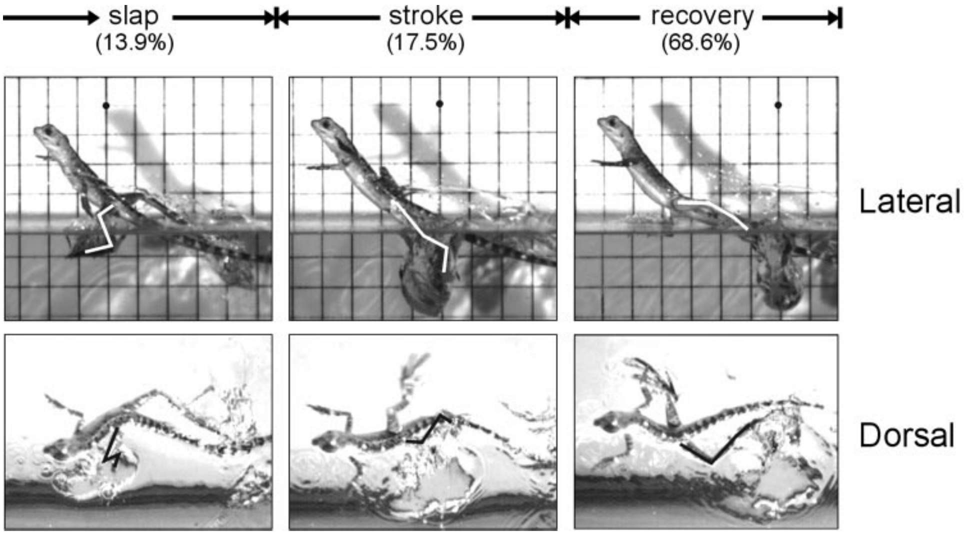

Fig. 1. Kinematic phases of a stride. Light-video images of dorsal and lateral views of an 18-g basilisk lizard running across the water surface. The white and black lines in the lateral and dorsal views, respectively, highlight the position of the hindlimb (thigh, calf, and foot, not including the toes). Each phase and its percent duration per total stride are shown above each pair of images. For this run, the positive *x* axis points anteriorly, the *y* axis points dorsally, and the *z* axis points to the right of the basilisk. The filled circle represents a fixed point of reference that does not move with the basilisk.

Kinematics. Knowledge of basilisk kinematics during each trial was essential for correlating force measurements with movements. Basilisks were induced to run across a 0.8-m-long water track. A plastic wall was mounted along the length of the track so it could be repositioned to narrow the width of the track and thereby better control the lizards' position during a run. Axes for analyses were oriented such that the positive *x* axis pointed in the direction of travel, the positive *y* axis pointed up, and the positive *z* axis was medial to the submerged foot. Lizards ran at sprint velocities within the range reported in another study (1.3–1.6 m/s; see ref. 7). Each running sequence was filmed with two synchronized high-speed Redlake Imaging (Morgan Hill, CA) PCI500 cameras operating at 250 frames per s with a shutter speed of 1/1,000 s. One camera filmed a dorsal view of the lizard through a mirror so we could determine the position of the lizards' foot relative to a laser light sheet illuminating the region of analysis in the water (see *DPIV*). The other camera filmed an ≈9 × 10-cm area of interest in the laser light sheet.

Basilisk lizard water-running kinematics are highly complex and are described in detail elsewhere (7). To facilitate analyses, each stride was divided into three phases based on foot kinematics: the slap, stroke, and recovery phases (7) (Fig. 1). The slap phase begins as the foot contacts the water and moves vertically downwards through the water. During the stroke phase, the foot sweeps primarily backwards and medially, ultimately shedding a vortex ring as it transitions into the recovery phase (Figs. 2 *c* and *d* and 3). The recovery phase completes a stride cycle, returning the foot to the start of slap.

The shed vortex ring is created by a transfer of momentum into the wake (13) and thus permits the calculation of forces produced by basilisks during the foot stroke. Because the slap and stroke phases serve as the propulsive phases of a stride, we were only interested in measuring the forces produced during these two phases.

Running sequences were determined to be acceptable only when the basilisk ran bipedally along the track such that its front limbs did not contact the water surface, and when there were no clear breaks in the basilisk's motion (e.g., running into the walls of the track or tripping during the run). As a result of these stringent selection criteria, we are confident that our data represent forces produced during true bipedal running across water. Data presented in this paper were taken from 24 runs by five individuals, with three to five runs per individual, per light sheet orientation.

DPIV. DPIV (14, 15) is a technique used for measuring forces produced in fluids that has recently been adapted from engineering for studies examining fish swimming (12, 13) and for robotic modeling of insect flight (16). This technique involves seeding the fluid with reflective particles and illuminating the area of interest with a thin laser sheet. Particle movement can then be traced and the forces calculated (13, 17).

The use of a laser light sheet for particle illumination places two limitations on data collection. First, the area of interest in this study was illuminated with a 6-W argon-ion laser focused into a light sheet ≈1 mm thick, effectively limiting visualization of fluid movement to a two-dimensional plane. To assess the three-dimensional structure of fluid movement during slap and the wake after stroke, we oriented the light sheet in separate experiments in three orthogonal planes: vertical (*x*–*y*), horizontal (*x*–*z*), and transverse (*y*–*z*) (Fig. 2*a*). We seeded the water in the track with near neutrally bouyant, reflective silver-coated glass spheres (mean diameter, 12 μm) to enable particle imaging. Because basilisks' limb movements are highly complex (7), for any single trial we were only able to record fluid motion during either the slap or the stroke phase. For a run to be acceptable for slap-force measurements, the foot needed to pass through the vertical or transverse light sheets. For stroke force determination, the stroke needed to be completed such that the shed vortex ring passed through the light sheet and was not subsequently obliterated by the tail, which dragged through the water as the basilisk ran.

The second limitation to light sheet DPIV was that we were only able to calculate peak force produced during each locomotor bout. During each sequence, the lizards' foot or vortex ring passed through the light sheet, briefly providing an accurate representation of maximal force as momentum is shed into the water in the form of a fully developed vortex ring. Reported forces (see below) are therefore time-averaged forces over the duration of foot movement. Any change in calculated force between frames resulted in part from differences in alignment of the vortex ring or foot with the plane of the light sheet as it passed

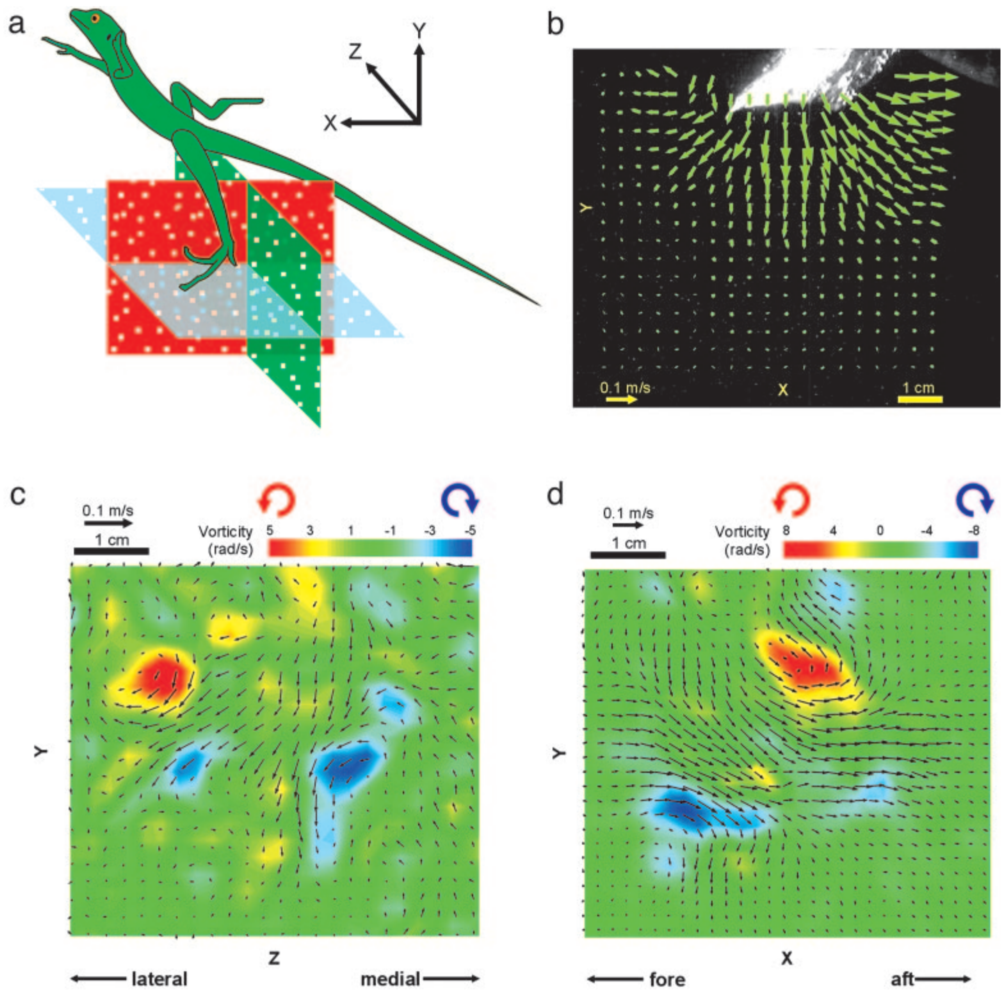

Fig. 2. Representative plots of particle movement during three sequences. (*a*) Schematic diagram of the positions of the three mutually orthogonal light sheets examined, relative to a running lizard. (*b*) Velocity of fluid movement during the initial slap phase. The underlying image shows the foot in the laser light sheet. (*c* and *d*) Color contour plots showing counterrotating centers of vorticity shed from the foot after the stroke phase. Red reflects strength of counterclockwise flow, and blue reflects strength of clockwise flow. Vector lengths in all plots reflect particle speed and direction. (*b* and *d*) Plots of fluid movement in the vertical light sheet. The lizard is shown running from right to left. (*c*) Plot of fluid movement in the transverse light sheet. The lizard is shown running into the page. In all panels, fluid motion is produced by the lizard's left foot.

through the sheet. Although this technique permits the calculation of a peak force, it does not allow for tracking the time course of force development through a slap or stroke. As a result, we report here only the time-averaged peak forces measured during the slap and stroke phases (Table 1).

Light sheet position relative to foot vortex position had no

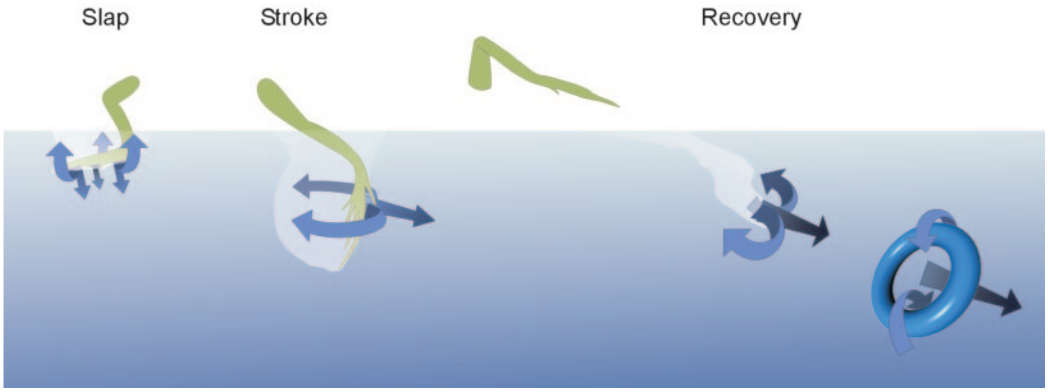

Fig. 3. Vortex ring formation during foot stroke. A schematic of vortex ring formation during the three kinematic phases of a stride. Note that the vortex ring is fully formed only after the foot has completed the stroke phase and has exited the water.

Table 1. Summary of single-leg peak reaction forces produced during a step

Direction	Slap, % (*n*)	Stroke, % (*n*)
Vertical	113 ± 8 (5)	39 ± 6 (3)
Fore–aft	63 ± 8 (5)	47 ± 14 (4)
Transverse	79 ± 17 (3)	−37 ± 13 (3)

Positive reaction forces point up, forward, and medial to the foot being analyzed. Results are presented as mean percent of body weight ± SEM, followed by the number of individuals analyzed in parentheses. Twenty-four total sequences were analyzed (two to six sequences per individual).

effect on calculated force magnitudes. The horizontal light sheet was initially positioned 6.8 cm below the water surface and gradually moved to 4.0 cm below the water surface between runs. A simple correlation analysis yielded no significant difference associating calculated force with light sheet depth (Bartlett χ^2, $P = 0.499$). Slap forces were calculated only in the vertical and transverse sheets because laser light reflection off the foot slapping through the horizontal sheet rendered the images unusable. Velocity components for each of the three planes were calculated by INSIGHT software (TSI, St. Paul) (12–15).

Force Calculations. Foot kinematics during slap and stroke phases are distinct (7); therefore, we analyzed data from each phase separately and with different methods. During the slap phase, we approximated the volume of water displaced by the foot as a moving cylindrical bolus of fluid. We were then able to calculate the generated time-averaged slap force from the total mean velocity (U, m/s) of cylinder expansion away from the foot as

$$F_{\text{slap}} = \frac{mU}{t}, \quad [1]$$

where m is the mass of the water in kilograms. Time t (in seconds) was determined to be the time period from first contact of the foot with the water surface to the analyzed frame.

Time-averaged stroke force generated in the fluid was estimated from each planar section by using

$$F = \rho\Gamma A/t, \quad [2]$$

where ρ is the density of water (998.23 kg/m^3 at 20°C), Γ (m^2/s) is the average circulation around the centers of vorticity, and A (m^2) is the projected area of the vortex ring on the light sheet (11, 13). Time, t, for stroke forces was the time from the start of stroke to the frame being analyzed.

Results and Discussion

The only other mechanistic investigations on basilisk lizard water running consisted of calculating the impulses produced at two phases meant to represent a basilisk step: at the instant a model foot impacted the water surface from a vertical drop, and during model deceleration as a result of hydrodynamic drag (5, 6). The model serves as a good approximation of the start of an actual step when DPIV cannot be used because this technique depends on fluid movement to determine momentum transfer. Beyond the moment the model foot contacts the water, however, the relevance of forces produced during passive model deceleration to basilisk lizard water running is limited. Foot movements when submerged are highly complex during actual water runs as basilisks actively sweep their foot through the water in three-dimensions (7). As a result, forces produced by a model passively decelerating only vertically through water because of hydrodynamic drag would not reflect additional thrust and side forces generated during an actual step.

The propulsive period of water running was represented by two kinematically distinct phases. During the slap phase of a step, the foot plunged vertically downwards, pushing water down and away from the foot while creating an air pocket surrounding the foot (Fig. 2*b*). During the stroke, the foot remained within this air pocket as water was pushed away from the ventral side of the foot and circulated cranially toward the dorsum. As the foot transitioned into the recovery phase, a vortex ring was shed (Fig. 2 *c* and *d*), representing a transfer of momentum into the fluid. This vortex ring was ≈3 cm in diameter with a central water jet directed medially, down, and opposite the running direction (Figs. 2 *c* and *d* and 3). The foot was extracted from the water before the air pocket collapsed.

Although the kinematics of water running in basilisks are variable (7), the force patterns were surprisingly consistent. Juveniles produced a large vertical slap force followed by a small vertical stroke force. On average, the vertical slap force was nearly three times as large as that produced during stroke, and exceeded body weight (Table 1). The stroke force magnitude was significantly less than body weight (Bonferroni-corrected t test, $P = 0.00$), suggesting that the initial impact force followed by more sustained slap force was sufficient to prevent the basilisk from sinking.

Our results revealed that, contrary to our expectations, similar magnitudes of fore–aft forces were generated during foot slap and stroke (Table 1), despite greater fore–aft translation of the foot during the stroke phase. Basilisks within the examined size range tend to slap the water with their foot in a slight toe down position (7). By contacting the water at an acute angle, the total generated force has both a vertical and fore–aft component. This, in combination with greater foot velocity during the slap phase (7) may account for similar fore–aft force contributions during the slap and stroke phases of a stride.

Transverse reaction forces were large (37–79% of body weight) and were directed medially during slap; the forces then switched directions and were directed laterally during stroke. Medial slap reaction forces on average were more than twice as large as lateral stroke reaction forces (Table 1). Forces produced during bipedal terrestrial locomotion have been examined only for animals with parasagittal limb motion. In these studies, transverse reaction forces are frequently not reported because they are of small magnitude and are variable (18). Where they are reported, transverse reaction forces are directed primarily medially during running (8, 18–20) and walking (21). Larger transverse ground reaction forces that are comparable with those reported in this study (≈20% body weight) were obtained for quadrupedal locomotion in iguanas and alligators, which exhibit large lateral body undulations (22). Transverse reaction forces during quadrupedal terrestrial locomotion were either directed medially (22) throughout the stride or switched lateral to medial (23), which is opposite that observed during bipedal water running in basilisk lizards.

Data from the present study suggest two complementary hypotheses for the significance of large transverse forces generated during water running by basilisk lizards. First, the large medial-then-lateral reaction forces aid in stabilizing the center of mass (CM). Greatest static stability is achieved when the CM is located between the supporting limbs, which delineates an ideal area of stability (24). Destabilization occurs when the CM moves close to or beyond the edges of the area of stability. Humans are known to control lateral balance and stability by increasing stride width (25) and presumably generating larger lateral forces to regain stability. Lizards running across water are faced with an unusual dynamic stability challenge: the yielding water surface and lateral body undulation while running cause the CM to experience large mediolateral excursions (23) toward and beyond the area of stability, thus causing the lizard to topple toward the supporting limb. By pushing laterally (producing medial reaction forces) as the CM translates toward the supporting limb and medially (producing lateral reaction forces) as the CM translates away from the supporting limb, the CM is forced back toward the center of stability. Second, the large transverse forces may reflect limitations imposed by anatomy or posture. The caudal fin in fishes is limited primarily to lateral bending, reflecting the muscular and skeletal structure of the tail (26–29). Iguanas and cockroaches, for example, also generate transverse forces, reflecting their sprawling posture. Cockroaches generate medial and lateral ground reaction forces (GRF) of ≈20% body weight (19). Iguanas generate a peak medial GRF of comparable magnitude but much smaller lateral GRF (22). When running across water, the basilisk lizard pelvic roll combined with sinking into a fluid surface forces the hindlimb to move medially, resulting in an extended medial stroke of the foot (7) and thus substantial transverse forces.

The mechanics of water running by basilisk lizards represent a novel mode of legged locomotion that cannot be accurately represented by the established spring-mass model of legged running (30, 31). Whereas hindlimb flexion occurs during the contact phase in terrestrial running, indicating energy storage in hindlimb tendons and ligaments, this does not occur during basilisk water running (7), which suggests that the hindlimb no longer functions like a spring but instead acts more like a piston, limited to only generating force during a step. The slap phase of a step is critical for generating sufficient vertical force to balance the basilisk's body weight, whereas both slap and stroke phases are important for generating fore–aft force. Finally, lateral undulation combined with continual sinking of the supporting limb results in the basilisk's toppling toward the supporting limb with each step. Our results suggest that the large transverse forces have two probable causes. The hindlimbs experience extreme medial excursions because of surface properties and anatomy and thus generate large lateral reaction forces. Transverse forces also act to move the CM back within the region of stability and are thus necessary for dynamic stabilization of locomotion on highly yielding surfaces, such as water.

We thank Andrew Biewener, Jim Glasheen, Farish Jenkins, Christoffer Johansson, Jimmy Liao, Russell Main, Jennifer Nauen, and Eric Tytell for many helpful discussions during this study. This study was funded by National Science Foundation Grants 9807021 and 0316675 (to G.V.L.), a National Science Foundation Graduate Research Fellowship (to S.T.H.), and a graduate student research grant from the Department of Organismic and Evolutionary Biology of Harvard University (to S.T.H.).

1. Bondarenko, L. V. (1995) *Entomol. Rev.* **74,** 161–165.
2. Hu, D. L., Chan, B. & Bush, J. W. M. (2003) *Nature* **424,** 663–666.
3. Suter, R. B. (1999) *Am. Sci.* **87,** 154–159.
4. Suter, R. B. & Wildman, H. (1999) *J. Exp. Biol.* **202,** 2771–2785.
5. Glasheen, J. W. & McMahon, T. A. (1996) *J. Exp. Biol.* **199,** 2611–2618.
6. Glasheen, J. W. & McMahon, T. A. (1996) *Nature* **380,** 340–342.
7. Hsieh, S. T. (2003) *J. Exp. Biol.* **206,** 4363–4377.
8. Cavagna, G. A. (1985) *J. Appl. Physiol.* **39,** 174–179.
9. Biewener, A. A. & Full, R. J. (1992) in *Biomechanics—Structures and Systems: A Practical Approach*, ed. Biewener, A. A. (Oxford Univ. Press, Oxford), pp. 45–73.
10. Winter, D. A. (1990) *Biomechanics and Motor Control of Human Movement* (Wiley, New York).
11. Dickinson, M. H. (1996) *Am. Zool.* **36,** 537–554.
12. Lauder, G. V. (2000) *Am. Zool.* **40,** 101–122.
13. Drucker, E. G. & Lauder, G. V. (1999) *J. Exp. Biol.* **202,** 2393–2412.
14. Raffel, M., Willert, C. & Kompenhans, J. (1998) *Particle Image Velocimetry: A Practical Guide* (Springer, Heidelberg).
15. Willert, C. E. & Gharib, M. (1991) *Exp. Fluids* **10,** 181–193.
16. Dickinson, M. H., Lehmann, F.-O. & Sane, S. P. (1999) *Science* **284,** 1954–1960.
17. Lauder, G. V. & Drucker, E. G. (2002) *News Physiol. Sci.* **17,** 235–240.
18. Munro, C. F., Miller, D. I. & Fuglevand, A. J. (1987) *J. Biomech.* **20,** 147–155.
19. Full, R. J. & Tu, M. S. (1990) *J. Exp. Biol.* **148,** 129–146.
20. Full, R. J. & Tu, M. S. (1991) *J. Exp. Biol.* **156,** 215–231.
21. Li, Y., Wang, W., Crompton, R. H. & Gunther, M. M. (2001) *J. Exp. Biol.* **204,** 47–58.
22. Blob, R. W. & Biewener, A. A. (2001) *J. Exp. Biol.* **204,** 1099–1122.
23. Farley, C. T. & Ko, T. C. (1997) *J. Exp. Biol.* **200,** 2177–2188.
24. Ting, L. H., Blickhan, R. & Full, R. J. (1994) *J. Exp. Biol.* **197,** 251–269.
25. Bauby, C. E. & Kuo, A. D. (2000) *J. Biomech.* **33,** 1433–1440.
26. Lauder, G. V. (1989) *Am. Zool.* **29,** 85–102.
27. Long, J. H. J. (1995) *Environ. Biol. Fishes* **44,** 199–211.
28. Nauen, J. C. & Lauder, G. V. (2002) *J. Exp. Biol.* **205,** 3271–3279.
29. Nauen, J. C. & Lauder, G. V. (2002) *J. Exp. Biol.* **205,** 1709–1724.
30. McMahon, T. A. & Greene, P. R. (1979) *J. Biomech.* **12,** 893–904.
31. Farley, C. T., Glasheen, J. W. & McMahon, T. A. (1993) *J. Exp. Biol.* **185,** 71–86.